Macromolecules **2009**, *42*, 8157–8164 **8157**
DOI: 10.1021/ma901397q

# Catalytic Polymerization in Dense $CO_2$ to Controlled Microstructure Polyethylenes

**Damien Guironnet, Inigo Göttker-Schnetmann, and Stefan Mecking***

*Department of Chemistry, Chair of Chemical Materials Science, University of Konstanz, D-78457 Konstanz, Germany*

*Received June 29, 2009; Revised Manuscript Received August 10, 2009*

ABSTRACT: A series of partially novel, ($\kappa^2$-*N,O*) Ni(II) methyl complexes coordinated by pyridine or *N,N,N′,N′*-tetramethylethylenediamine (tmeda), based on different $\kappa^2$-*N,O*-chelating salicylaldimines, 2,6-diisopropylanilinotropone, and a ketoenamine, were studied as precatalysts for olefin polymerization in dense carbon dioxide. Bis(trifluoromethyl)phenyl substituents promote solubility in the $CO_2$ reaction medium, as quantified by solubility studies of the free N,OH ligands over a range of $CO_2$ densities ($\rho$ = 0.2−0.9 g mL$^{-1}$) at 25 and 50 °C and thus enhance catalyst activities. By appropriate choice of the catalyst precursor and polymerization reaction conditions ($CO_2$ density, ethylene concentration, and temperature), strictly linear polyethylene with high molecular weight is obtained (< 1 branch/1000 carbon atoms, $M_w = 10^6$ g mol$^{-1}$; $M_w/M_n = 2$) which displays typical thermal characteristics and density of ultrahigh molecular weight polyethylene. Copolymerization with 1-hexene, and particularly with norbornene, allows for controlling polymer crystallinity and melting temperature down to $\chi < 20\%$ and $T_m < 70$ °C.

## Introduction

Dense carbon dioxide, that is, liquid or supercritical carbon dioxide ($scCO_2$), offers unique properties as a reaction medium.[1] By comparatively minor variations of temperature and/or pressure, the density and thus solvent properties of the medium can be varied over a wide range. Obviously, the volatility at ambient conditions enables a facile removal of $CO_2$ from the reaction mixture. The unique properties of $CO_2$ can also be employed in polymerization processes to control polymer morphologies.[2] Consequently, polymerization in dense carbon dioxide has attracted considerable interest. While free-radical polymerization[2,3] of a variety of monomers has been studied under heterogeneous conditions, either as precipitation, dispersion, or emulsion polymerization, cationic[4] and catalytic polymerizations are also well-known. Epoxide−carbon dioxide[5] and ethylene−carbon monoxide copolymerization,[6] phenylacetylene polymerization,[7] and ring-opening metathesis polymerization of norbornene and derivatives[8] have been reported.

Remarkable in view of the paramount importance of polyolefin materials, olefin polymerization in $scCO_2$ has found comparatively little attention. Ethylene polymerization in $scCO_2$ with cationic Pd(II) diimine catalysts,[9] analogous to polymerization in organic solvents with these catalysts, afforded highly branched amorphous polyethylenes invariably.[10] $CO_2$-soluble neutral Ni(II) salicylaldiminato complexes have been investigated preliminarily, with low ethylene concentrations limited by the setup employed. In the course of this study linear semicrystalline polyethylene with molecular weight limited to $M_n = 2.4 \times 10^4$ g mol$^{-1}$ and a moderate degree of branching of ca. 10−30 methyl branches per 1000 carbons were obtained.[11] The aforementioned predominance of polyolefin materials is based, for the case of polyethylenes, on linear homopolymers and copolymers with variable degrees of crystallinity. We now give a comprehensive account of the preparation of such materials, with homopolymer molecular weights approaching the ultrahigh molecular weight regime, in dense $CO_2$. For this purpose a range of partially novel, well-defined neutral Ni(II) catalyst[12,13] precursors is studied concerning their solubility and polymerization properties in $CO_2$. This type of late transition metal catalyst[14] was chosen as it is particularly tolerant toward polar reaction media.[13e,15,16]

*Corresponding author. E-mail: stefan.mecking@uni-konstanz.de.

## Results and Discussion

**Catalyst Precursors.** *Bidentate Ligands*. The choice of catalysts studied was guided by their anticipated ability to form certain microstructures based on their catalytic behavior in hydrocarbon solvents, particularly linear polymers of high molecular weight and copolymers, and solubility issues. $CO_2$ is a rather poor solvent for metal complexes under reasonable conditions (< 100 °C and < 1000 bar). This has been overcome by the introduction of long perfluoroalkyl chains, which can provide solubility in supercritical carbon dioxide. However, the synthesis of corresponding ligands requires time-consuming multistep procedures.[17] Alternatively, a large number of trifluoromethyl moieties can provide solubility in $scCO_2$. At the same time, the electron-withdrawing nature of such substituents, which affects the metal center even if the substituents are in a remote position of the active species, promotes formation of linear polyethylene and increases catalyst stability.[13g,13l−13n] This can be traced to a reduced propensity for $\beta$-hydride elimination with increasing electrophilic nature of the metal sites within a given class of catalysts. $\beta$-Hydride elimination is a key step of both branch formation in ethylene homopolymerization and of chain transfer. Also, the Ni(II) hydride species formed undergo bimolecular reductive elimination with Ni(II) alkyl species as a relevant decomposition route.[16] Salicylaldimines **1b**−**d**,[18] anilinotropone **3**,[13d,36] and ketoenamine **5**[13m] were prepared by reported procedures. For **1a**,[18] containing eight trifluoromethyl groups, a shorter and improved two-step synthesis was developed (Scheme 1). Condensation of 3,5-diiodosalicylaldehyde with 2,6-dibromoaniline followed by simultaneous 4-fold Suzuki coupling



Published on Web 08/24/2009

**Scheme 1. Synthesis of Salicylaldimine**

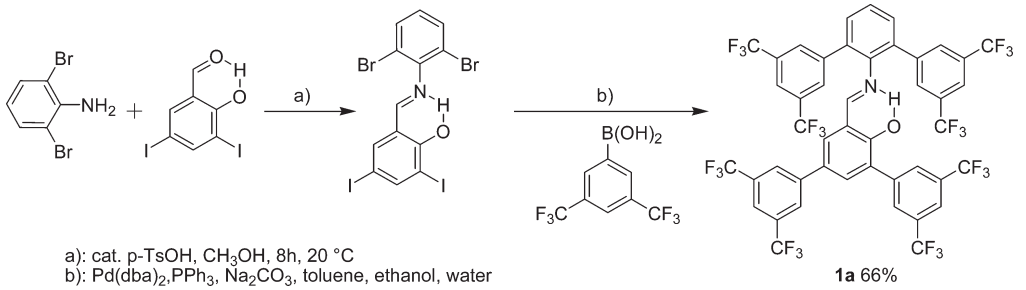


with 3,5-bis(trifluoromethyl)phenylboronic acid afforded **1a** in 66% overall yield.

*Solubility in Dense $CO_2$.* The solubility of selected ligands in dense $CO_2$ was investigated by means of a custom-made infrared spectroscopy setup at the CNRS in Bordeaux.[19] The molar extinction coefficients ($\varepsilon$) of characteristic vibration bands were calculated from FT-IR spectra collected at high $CO_2$ density (completely dissolved substrate). Solubilities were determined from spectra acquired at variable pressures (from 6 to 35 MPa) along the 25 and 50 °C isotherms by assuming ($\varepsilon$) to be independent of pressure and temperature, which appears reasonable given that also no significant band shifts were observed.

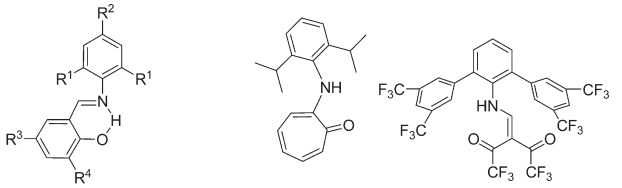

**1a**: $R^1 = R^3 = R^4 = 3,5\text{-}(CF_3)_2C_6H_3$; $R^2 = H$
**1b**: $R^1 = R^2 = R^3 = R^4 = 3,5\text{-}(CF_3)_2C_6H_3$
**1c**: $R^1 = {}^i$Pr; $R^2 = R^3 = H$; $R^4 = 9$-anthryl
**1d**: $R^1 = 3,5\text{-}(CF_3)_2C_6H_3$; $R^2 = H$; $R^3 = R^4 = I$

**3**

**5**

As anticipated, salicylaldimine **1a** and ketoenamine **5** with a high fluorine content are highly soluble even at a moderate density (Table 1). At $\rho = 0.70$ g mL$^{-1}$, solubility of **1a** is ca. 3.6 mmol L$^{-1}$, and solubility of **5** exceeds 9 mmol L$^{-1}$. By comparison to these highly fluorinated compounds, **1c** is much less soluble even at high density (ca. 0.12 mmol L$^{-1}$ at $\rho = 0.87$ g mL$^{-1}$), though absolute solubility is reasonably high. Solubilities are not significantly dependent upon temperature in the range studied, but rather on the medium density; at higher temperature the solubility equilibrium was merely reached faster. The solubilities of most ligands studied (**1a**, **1d**, **5**) exceed the usual concentration of catalyst during the polymerization experiments (ca. $3 \times 10^{-4}$ mol L$^{-1}$). Solubility of the corresponding catalyst precursors (vide infra) is somewhat lower. For example, complex **2d-pyr** is incompletely soluble in the medium under polymerization conditions ($\rho = 1.01$ g mL$^{-1}$), as observed through the sapphire window of the polymerization autoclave (Figure 2a). Nonetheless, the solubilities determined for the corresponding ligands are a useful qualitative indicator of the relative miscibility of the different polymerization active sites with the $CO_2$ reaction medium.

*Synthesis and Characterization of Neutral Nickel(II) Complexes.* Two types of complexes, varying in the labile coordinating ligand stabilizing the catalyst precursors, were prepared for polymerization studies. ($\kappa^2$-*N,O*)-salicylaldiminato nickel(II) methyl pyridine complexes **2a-d-pyr**[13l] and ($\kappa^2$-*N,O*)-enolatoiminenickel(II) methyl-

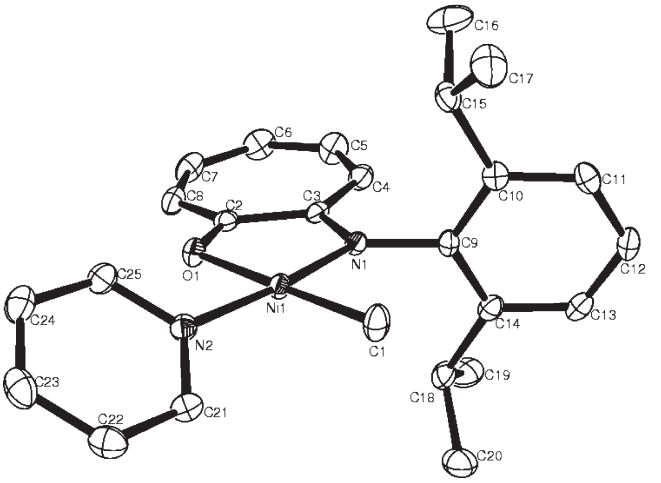

**Figure 1.** ORTEP plot of **4-pyr**. Ellipsoids are shown with 50% probability. Hydrogen atoms are omitted for clarity.

pyridine complex **6-pyr**[13m] were prepared according to reported procedures.

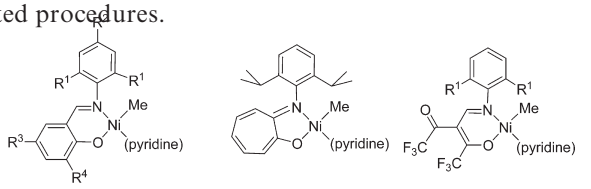

**2a-pyr**: $R^1 = R^3 = R^4 = 3,5\text{-}(CF_3)_2C_6H_3$; $R^2 = H$
**2b-pyr**: $R^1 = R^2 = R^3 = R^4 = 3,5\text{-}(CF_3)_2C_6H_3$
**2c-pyr**: $R^1 = {}^i$Pr; $R^2 = R^3 = H$; $R^4 = 9$-anthryl
**2d-pyr**: $R^1 = 3,5\text{-}(CF_3)_2C_6H_3$; $R^2 = H$; $R^3 = R^4 = I$

**4-pyr**

**6-pyr** ($R^1 = 3,5\text{-}(CF_3)_2\text{-}(C_6H_3)$)

The 2-(2,6-diisopropylanilino)tropone nickel(II) methyl pyridine complex (eq 1, **4-pyr**) was prepared by reaction of **3** with [(pyridine)$_2$NiMe$_2$] at −30 °C in Et$_2$O in 85% yield (eq 1). A single-crystal X-ray analysis confirmed the structure of **4-pyr** (Figure 1). The coordination geometry around the Ni(II) center is square-planar, with the methyl group cis to the *N*-aryl moiety. This resembles the geometry of the analogous ($\kappa^2$-*N,O*)-2,6-diisopropylanilinotropone nickel(II) phenyl triphenylphosphine.[13d]

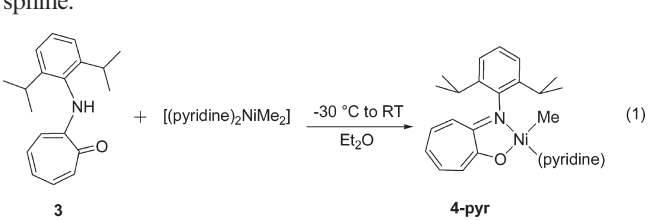


**3** **4-pyr**

By comparison to pyridine, the tertiary amine *N,N,N′,N′*-tetramethylethylenediamine (tmeda), which is introduced when employing [(tmeda)NiMe$_2$] as a Ni(II) source, is more

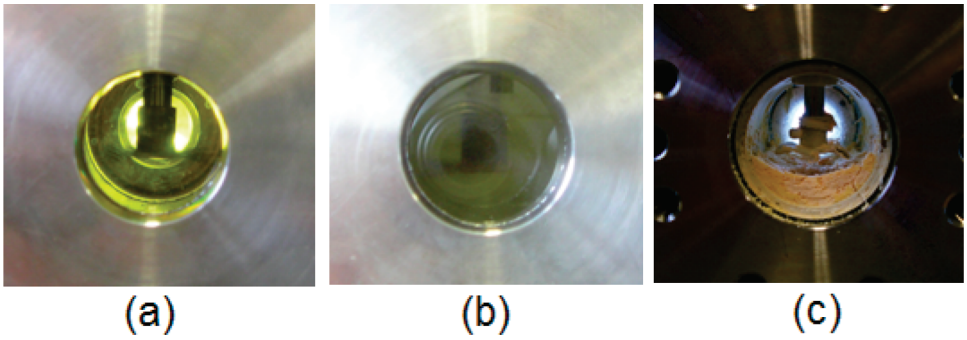


**Figure 2.** Photographs of the high-pressure autoclave during polymerization: (a) **2a-pyr** dissolved in $scCO_2$ (b) directly after addition of ethylene; (c) polymer formed after releasing the pressure.

**Table 1. Solubility of Selected Compounds in $scCO_2$ at Different Densities**[a]

| | solubility of compounds [mmol $L^{-1}$] | | | |
|---|---|---|---|---|
| density [g $mL^{-1}$] | **1a** | **1c** | **1d** | **5** |
| 0.22 | 0.02 | 0 | 0 | 0.1 |
| 0.38 | 0.21 | 0.01 | 0.08 | 7.35 |
| 0.70 | 3.63 | 0.05 | 1.76 | > 9.2 |
| 0.78 | > 4 | 0.09 | > 3.8 | n.d. |
| 0.84 | n.d. | 0.11 | n.d. | n.d. |
| 0.87 | n.d. | 0.12 | n.d. | n.d. |

[a] 50 °C, from 6 to 35 MPa; n.d. = not determined.

labile.[20] This enhances polymerization activities, as a coordination site for binding of olefin substrate is more readily provided. Because of the multiple coordination modes of tmeda ($\kappa^1$, $\kappa^2$), tmeda adducts are a mixture of various Ni−Me species, other than the well-defined pyridine adducts, as reported in detail for **2d-tmeda**.[21] Complexes **2a-d-tmeda** were prepared by reaction of [(tmeda)$NiMe_2$] with a substoichiometric amount of the respective salicylaldimine **1a-d** in cold benzene (eq 2). After stirring until excess [(tmeda)$NiMe_2$] had decomposed (60 min), **2a-d-tmeda** were isolated by filtering off nickel black and removing all volatiles in vacuum.[22] The resulting solids were employed as catalyst precursors without further characterization.

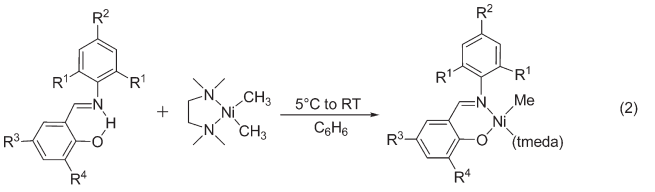


(2)

**2a-tmeda**: $R^1 = R^3 = R^4 = 3,5\text{-}(CF_3)_2C_6H_3$; $R^2$ = H
**2b-tmeda**: $R^1 = R^2 = R^3 = R^4 = 3,5\text{-}(CF_3)_2C_6H_3$
**2c-tmeda**: $R^1 = {}^i$Pr; $R^2 = R^3$ = H; $R^4$ = 9-anthryl
**2d-tmeda**: $R^1 = 3,5\text{-}(CF_3)_2C_6H_3$; $R^2$ = H; $R^3 = R^4$ = I

**Polymerization of Ethylene.** Ethylene polymerizations with **2a-d-pyr**, **4-pyr**, and **6-pyr** were performed at 50 °C in supercritical carbon dioxide (Table 2). Surprisingly, in view of the activity and stability of polymerization with **4-pyr** in toluene as reaction medium, only traces of polymer were obtained reproducibly with **4-pyr** in the attempted polymerization in $CO_2$, presumably due to rapid decomposition of the catalytically active species.[23] In contrast, an activity of up to $10^4$ mol $(C_2H_4)$ mol $(Ni)^{-1}$ $h^{-1}$ was observed for **6-pyr** and **2c-pyr**.[24] It is worth noting that the activity of **6-pyr** in $scCO_2$ resembles the activity observed in toluene as an organic solvent under otherwise similar conditions (50 °C, in $scCO_2$: $2.3 \times 10^4$ TO $h^{-1}$; in toluene under 40 bar ethylene $2.4 \times 10^4$ TO $h^{-1}$). This observation can be correlated with the high solubility in $scCO_2$ of the corresponding ligand **5** (Table 1). In all polymerization studies, immediate precipitation of polymer was observed upon addition of ethylene (Figure 2). A sufficient high miscibility of the active sites with the $CO_2$ reaction medium may sustain accessibility for the olefin substrate. Polyethylene molecular weights are high ($M_w \approx 10^5$ g $mol^{-1}$, $M_w/M_n \approx 2$; Table 2), with a low to moderate degree of branching (vide infra).

Polymer of very high molecular weight ($M_w$ up to $10^6$ g $mol^{-1}$) was accessible at a polymerization temperature of 5 °C (Figure 3). At this temperature, hindered dissociation of pyridine strongly limits the activities of the pyridine complexes. The tmeda adducts **2a-d**, however, display high productivities of $10^4$ TO over a 12 h experiment also at 5 °C (entries 2-3, 2-6, 2-8, and 2-10). Overall, polymer molecular weights do not differ dramatically by comparison to polymerization in toluene under similar conditions (specifically polymerization temperature, monomer concentration).[13l,25]

**Polyethylene Microstructure.** The degree of branching of selected ethylene homopolymers was determined by quantitative high-temperature $^{13}C$ NMR spectroscopy (Table 3). While materials obtained with the salicylaldiminato complexes **2a,b** at a polymerization temperature of 20 °C or higher possess a low degree of branching (entries 2-1 and 2-2), polymers formed at 5 °C are strictly linear with less than one branch per 1000 carbon atoms (entries 2-3, 2-6, and 2-10). In accordance with the observed behavior in organic solvent, the enolatoimine complex **6-pyr** has a higher tendency for "chain walking" as evidenced by the formation of moderately branched polymer with up to 11 methyl branches per 1000 carbon atoms (entry 2-12). The presence or absence of these irregularities in the polymer backbone is reflected by the melting temperatures and crystallinity of the polymers, as determined by DSC (Table 3). Notably, the strictly linear, high molecular weight polymers demonstrate thermal properties typical of ultrahigh molecular weight polyethylene (UHMWPE).[27,28] High peak melting temperatures (141−142 °C) and heats of fusion ($\Delta H_m \approx 190$ J $g^{-1}$, corresponding to a degree of crystallinity $\chi = 64\%$) are observed for the nascent polymer in the first heating cycle (Figue 3), and these values are significantly reduced in the second heating cycle ($T_m = 135-136$ °C, $\Delta H_m \approx 150$ J $g^{-1}$). The large differences between the crystallinity of the nascent polymer and the polymer crystallized from the melt are due to chain entanglement in the melt hindering recrystallization. Also, densities are low by comparison to typical HDPE, as expected for ultrahigh molecular weight polyethylene.[29]

**Copolymerization.** Introduction of branches by copolymerization of ethylene with 1-olefins is widely applied to control the crystallinity of polyolefins. Because of the

**Table 2. Polymerization of Ethylene in Dense Carbon Dioxide**

| entry | catalyst | Ni [μmol] | approx density[a] [g mL$^{-1}$] | $C_2H_4$ [g] | temp [°C] | $t$ [h] | TON[b] | yield [g PE] | $M_w$[c] [g mol$^{-1}$] | $M_w/M_n$[c] | $T_m$[d] [°C] | $\chi$[d] [%] |
|---|---|---|---|---|---|---|---|---|---|---|---|---|
| 2-1 | **2a-pyr** | 15 | 1.00 | 9 | 50 | 0.5 | 2930 | 1.23 | $3.1 \times 10^5$ | 2.1 | 125 | 49 |
| 2-2 | **2a-tmeda** | 10 | 1.08 | 12 | 20 | 1 | 4800 | 1.34 | $2.5 \times 10^5$ | 2.8 | 125 | 47 |
| 2-3 | **2a-tmeda** | 10 | 1.12 | 15 | 5 | 12 | 14600 | 4.08 | $1.0 \times 10^6$ | 1.8 | 136 | 52 |
| 2-4 | **2b-pyr** | 10 | 1.00 | 9 | 50 | 1 | 7290 | 2.04 | $1.1 \times 10^5$ | 2.0 | 119 | 46 |
| 2-5 | **2b-pyr** | 10 | 1.08 | 12 | 20 | 12 | 1570 | 0.44 | $5.1 \times 10^5$ | 8.9 | 133 | 56 |
| 2-6 | **2b-tmeda** | 10 | 1.12 | 15 | 5 | 2 | 11300 | 3.17 | $6.3 \times 10^5$ | 1.7 | 135 | 51 |
| 2-7 | **2c-pyr** | 10 | 1.00 | 9 | 50 | 1 | 10890 | 3.05 | $2.7 \times 10^5$ | 1.8 | 132 | 53 |
| 2-8 | **2c-tmeda** | 10 | 1.12 | 15 | 5 | 12 | 14500 | 4.06 | $7.9 \times 10^5$ | 1.8 | 137 | 52 |
| 2-9 | **2d-pyr** | 10 | 1.00 | 9 | 50 | 0.5 | 3610 | 1.01 | $2.7 \times 10^5$ | 2.2 | 130 | 51 |
| 2-10 | **2d-tmeda** | 12 | 1.12 | 15 | 5 | 12 | 9430 | 3.17 | $9.3 \times 10^5$ | 1.8 | 135 | 50 |
| 2-11 | **4-pyr** | 10 | 1.00 | 9 | 50 | 1 | | traces | $3.7 \times 10^5$ | 4.2 | 121 | 44 |
| 2-12 | **6-pyr** | 6 | 1.00 | 9 | 50 | 1 | 23200 | 3.75 | $1.8 \times 10^5$ | 1.9 | 117 | 43 |

[a] Density of neat carbon dioxide at this temperature and pressure (65 MPa) according to ref 26. [b] TON in mol ($C_2H_4$) mol (Ni)$^{-1}$. [c] Determined by GPC, referenced to linear polyethylene. [d] Determined by DSC from the second heating trace.

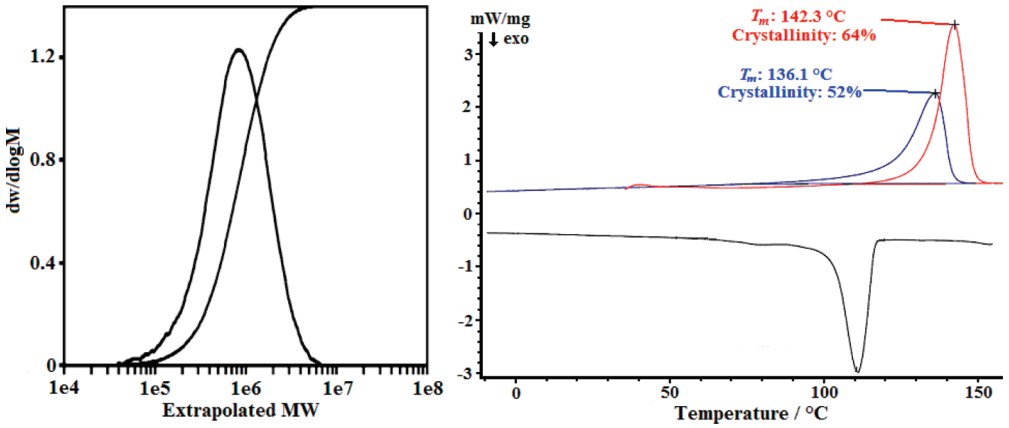


**Figure 3.** GPC trace (left) and DSC diagram (right, red first heating trace; blue, second heating trace) of polyethylene prepared with catalyst precursor **2c-pyr** at 5 °C (entry 2-3).

**Table 3. Polymer Microstructures**

| entry | precatalyst | $M_w$[a] [g mol$^{-1}$] | $M_w/M_n$[a] | $T_m$[b] [°C] | $T_m$[c] [°C] | $\chi$[b] [%] | $\chi$[c] [%] | branches /1000C[d] | density[e] |
|---|---|---|---|---|---|---|---|---|---|
| 2-1 | **2a-pyr** | $3.1 \times 10^5$ | 2.1 | 130 | 125 | 54 | 49 | 4 | |
| 2-2 | **2a-tmeda** | $2.5 \times 10^5$ | 2.8 | 133 | 125 | 56 | 47 | 4 | |
| 2-3 | **2a-tmeda** | $1.0 \times 10^6$ | 1.8 | 142 | 136 | 64 | 52 | < 1 | 0.927 |
| 2-6 | **2b-tmeda** | $6.3 \times 10^5$ | 1.7 | 140 | 135 | 64 | 51 | < 1 | 0.932 |
| 2-10 | **2d-tmeda** | $9.3 \times 10^5$ | 1.8 | 141 | 135 | 64 | 50 | < 1 | 0.931 |
| 2-12 | **6-pyr** | $1.8 \times 10^5$ | 1.9 | 120 | 117 | 47 | 43 | 11 | 0.923 |

[a] Determined by GPC, referenced to linear polyethylene standards. [b] Determined by DSC from the first heating trace. [c] Determined by DSC from the second heating trace. [d] Determined by $^{13}C$ NMR, exclusively methyl branches. [e] Determined according to ISO 1183 via the immersion method.[30]

aforementioned ability of **2a-pyr** to form high molecular weight ethylene homopolymers in $scCO_2$, and the capability of **6-pyr** to insert also into a secondary alkyl species, as evidenced by the methyl branching of the ethylene homopolymer, these catalyst precursors were selected for studies of copolymerization (Table 4). In addition to 1-hexene (H), the strained cyclic norbornene (NB) was employed as a comonomer. Comonomer incorporation resulted in reduced catalyst activities by comparison to ethylene homopolymerization (approximately an order of magnitude lower) due to a slow insertion of the bulky comonomer or slow ethylene insertion after comonomer insertion. Also, polymer molecular weights are reduced by comparison to the homopolymers formed under otherwise identical conditions. For a given set of reaction conditions, the degree of incorporation, determined by quantitative $^{13}C$ NMR spectroscopy (Figure 4), does not differ strongly between the two different catalysts investigated. Overall, the relative reactivity toward the comonomers, as reflected by the copolymer composition, resembles the behavior of neutral nickel(II) complexes in organic solvents.[18,31,32] Ethylene incorporation is much preferred over 1-olefin incorporation; under the conditions studied the mole fraction of hexene-derived repeat units in the copolymers vs mole fraction in the reaction mixture amounts to ca. $X_{1\text{-hexene}}/x_{1\text{-hexene}} \approx 0.1$. By contrast, norbornene is incorporated more efficiently with only a slight preference for ethylene. This enables a control of polymer crystallinity and melting temperature over a wide range, down to $\chi < 20\%$ and a peak melting temperature $T_m < 70$ °C. At the same time, molecular weights are sustained in the $10^4$ g mol$^{-1}$ regime (Table 4 and Figure 5). In addition to the branches formed by comonomer incorporation, all copolymers possess a similar degree of ethylene-derived methyl branches as the corresponding homopolymers, as a result of chain walking (Figure 4 and Table 4). Note that the degree of ethylene-derived branching is higher by comparison to ethylene homopolymer prepared with the same catalyst precursor and at the same temperature due to a higher ethylene concentration in the homopolymerization.

**Polymer Morphology.** Polymerization of ethylene in carbon dioxide resembles a precipitation polymerization process. Upon venting the high-pressure reactor carefully

**Table 4. Copolymerization of Ethylene with 1-Hexene and Norbornene in Dense Carbon Dioxide[a]**

| entry | complex | Ni [μmol] | $C_2H_4$ [g] | $x_{comon}$[b] | TON[c] | polymer yield [g] | $M_w$[d] [$10^3$ g mol$^{-1}$] | $M_w/M_n$[d] | $T_m$[e] [°C] | $\chi$[e] [%] | $X_{comon}$[f] [mol %] | ethylene-derived branches/ 1000C[g] |
|---|---|---|---|---|---|---|---|---|---|---|---|---|
| 4-1 | **6-pyr** | 10 | 3 | 0.27 H | 4280 | 1.1 | 15.0 | 5.7 | 105 | 36 | 1.0 | 17 |
| 4-2 | **6-pyr** | 10 | 3 | 0.09 NB | 780 | 0.25 | 27.3 | 2.4 | 71 | 23 | 6.0 | 11 |
| 4-4 | **6-pyr** | 10 | 7 | 0.04 NB | 2000 | 0.60 | 16.4 | 7.0 | 94 | 24 | 2.5 | 8 |
| 4-5 | **2a-pyr** | 20 | 7 | 0.04 NB | 850 | 0.52 | 5.7 | 6.4 | 58 | <20 | 4.0 | 10 |
| 4-6 | **2a-pyr** | 15 | 3 | 0.07 NB | 350 | 0.15 | 8.3 | 4.2 | 88 | <20 | 2.5 | 13 |
| 4-7 | **2a-pyr** | 17 | 5 | 0.15 H | 1860 | 0.90 | 11.4 | 3.8 | 108 | 39 | 1.0 | 16 |
| 4-8 | **2a-pyr** | 20 | 3 | 0.31 H | 1030 | 0.90 | 1.8 | 4.9 | 79 | 27 | 2.5 | 28 |

[a] Reaction conditions: 60 mL of carbon dioxide at 20 MPa and 50 °C initially, compressed to 30 MPa by decrease of volume, followed by addition of ethylene at constant pressure, and compression to 65 MPa by decrease of volume; polymerization temperature 50 °C; $CO_2$ density ca. 1.00 g mL$^{-1}$. [b] Initial molar fraction of comonomer in reaction mixture. [c] TON in mol (olefin) mol (Ni)$^{-1}$. [d] Determined by GPC, referenced to linear polyethylene. [e] Determined by DSC from the second heating trace. [f] Molar fraction of comonomer repeat units in polymer. [g] Branches determined by $^{13}$C NMR.

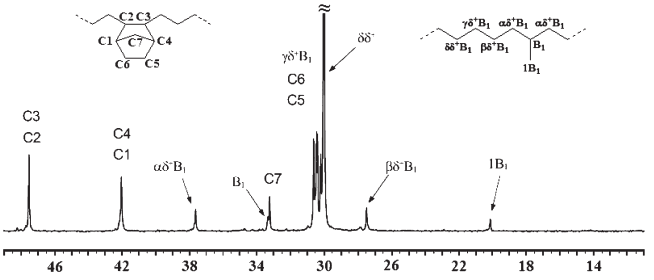


**Figure 4.** $^{13}$C NMR spectrum of an ethylene/norbornene copolymer (100 MHz; 130 °C; $C_2D_2Cl_4$). Polymer prepared with catalyst precursor **6-pyr** (entry 4-2).

after the desired polymerization time, the polymer is obtained directly as a dry powder (Figure 2c). The polyethylene particles were studied by transmission electron microscopy (Figure 6). Despite the presence of larger agglomerates, it is evident that the material consists of very small primary particles of only a few tens of nanometers in size. This is likely due to a poor swellability of the polymer with $scCO_2$, resulting in precipitation of the nascent polymer particles at a very early stage.

**Summary and Conclusions.** A series of neutral ($\kappa^2$-*N,O*) nickel methyl complexes based on three different classes of bidentate ligands were investigated for olefin polymerization in $scCO_2$. The enhancement of solubility by multiple trifluoromethyl moieties was quantified. Enolatoimine **5** with six trifluoromethyl groups exhibits a high solubility already at mild conditions (solubility >9.2 mmol L$^{-1}$ at $\rho$ = 0.70 g mL$^{-1}$). The respective catalyst precursor **6-pyr** polymerizes ethylene in $scCO_2$ with an unprecedented catalyst activity ($2.3 \times 10^4$ mol ($C_2H_4$) mol (Ni)$^{-1}$ h$^{-1}$), which resembles activities observed in toluene as an organic solvent. This is likely enhanced by the high miscibility of the active sites with the $scCO_2$ reaction medium, which aids the access of olefin substrate. Overall, the polymerization studies with various catalysts indicate no general tendency for $CO_2$ to interact with neutral Ni(II) complexes in a disfavorable fashion, e.g., by blocking coordination sites for substrates or promoting irreversible deactivation reactions.[33] With appropriate catalyst precursors and at suitable reaction conditions, that is, monomer concentration, medium density, and temperature, strictly linear polyethylene with less than one branch per 1000 carbon atoms and properties typical of ultrahigh molecular weight polyethylene are obtained. Copolymerization with norbornene, incorporation of which is not much disfavored toward ethylene incorporation, enables a control of polymer crystallinity and melting temperature, down to $\chi$ < 20% and $T_m$ < 70 °C. While comonomer incorporation occurs at the expense of molecular weights, the latter remain in the regime of several $10^4$ g mol$^{-1}$. The linear polyethylene formed consists of primary particles of only several 10 nm size, which can be related to a rapid precipitation during the polymerization reaction due to immiscibility of the polymer with $scCO_2$.

## Experimental Section

**Materials and General Considerations.** Unless noted otherwise, all manipulations of metal complexes were carried out under an inert atmosphere using standard glovebox or Schlenk techniques. All glassware was flame-dried under vacuum before use. Toluene and benzene were distilled from sodium and diethyl ether from sodium/ketyl benzophenone under argon. Pyridine and pentane were distilled from $CaH_2$. Demineralized water was distilled under nitrogen. Ethylene (3.5 grade) and carbon dioxide (5.5 grade) supplied by Praxair and Air Liquid were used as received, respectively. All other solvents were commercial grade. [(tmeda)Ni($CH_3$)$_2$][34] was purchased from MCat (Konstanz, Germany) and stored at −30 °C in a glovebox prior to use. [(pyridine)$_2$Ni($CH_3$)$_2$][35] was synthesized by a modified literature procedure and stored at −30 °C in a glovebox. 3,5-Bis[3,5-di(trifluoromethyl)phenyl]salicylaldehyde,[18] 2,4,6-tris{3,5-di(trifluoromethyl)phenyl}aniline,[25] ligands **1d**,[13g] **3**,[36] and **5**,[13m] and complexes **2a-pyr**,[18] **2d-pyr**,[13g] and **6-pyr**[13m] were prepared according to literature procedures.

NMR spectra were recorded on a Varian Unity INOVA 400 or on a Bruker Avance DRX 600 spectrometer. $^1$H and $^{13}$C NMR chemical shifts were referenced to the solvent signal. The identity and purity of metal complexes were established by $^1$H and $^{13}$C NMR and elemental analysis. NMR assignments were confirmed by 1H,$^1$H gCOSY, $^1$H,$^{13}$C gHSQC, and $^1$H,$^{13}$C gHMBC experiments. High-temperature NMR measurements of polyethylenes were performed in 1,1,2,2-tetrachloroethane-$d_2$ at 130 °C. Gel permeation chromatography (GPC) was carried out in 1,2,4-trichlorobenzene at 160 °C on a Polymer Laboratories 220 instrument equipped with Olexis columns with differential refractive index, viscosity, and light scattering (15° and 90°) detectors. Data reported were determined via universal calibration (for samples with $M_n$ < $10^5$ g mol$^{-1}$) and triple detection ($M_n$ > $10^5$ g mol$^{-1}$). Both methods were in good agreement with one another. Differential scanning calorimetry (DSC) was performed on a Netzsch Phoenix 204 F1 at a heating rate of 10 K min$^{-1}$. DSC data reported are from second heating cycles, unless noted otherwise. Polymer crystallinities were calculated based on a melt enthalpy of 293 J g$^{-1}$ for 100% crystalline polyethylene. Elemental analyses were performed up to 950 °C on an Elementar Vario EL. Densities of polyethylenes were determined according to ISO 1183 via the immersion method. The sample, compressed as a pellet, is weighed in air and then weighed when immersed in distilled water at 23 °C using a sinker and wire to hold the sample completely submerged as required.

**2-((2,6-Dibromophenylimino)methyl)-4,6-diiodophenol.** To a solution of 3,5-diiodosalicylaldehyde (2.7 mmol, 1.00 g) in methanol (10 mL), 2,6-dibromoaniline (2.7 mmol, 0.68 g) and

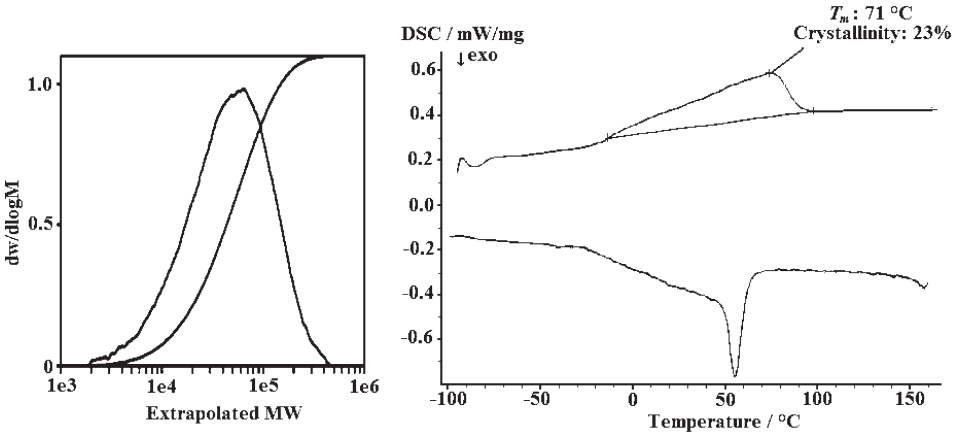


**Figure 5.** GPC trace (left) and DSC diagram (right) of ethylene−norbornene copolymer prepared with catalyst precursor **6-pyr** (entry 4-2).

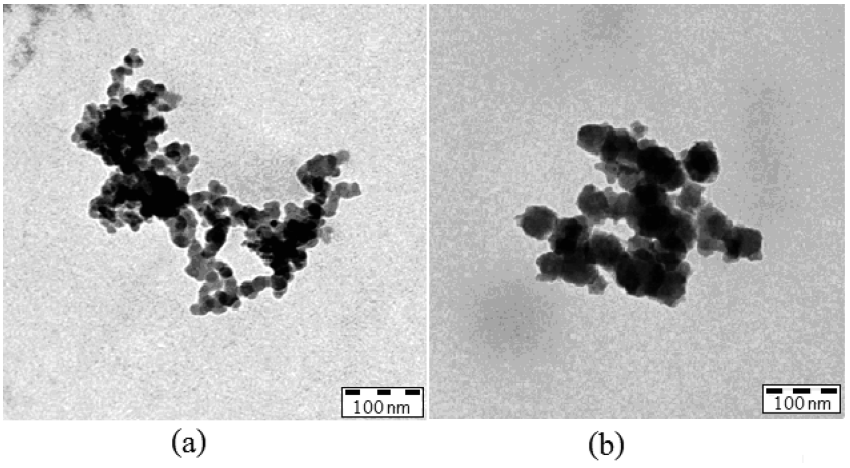


**Figure 6.** TEM images of polyethylene particles produced in $scCO_2$ at 50 °C and 65 MPa.

a catalytic amount of *p*-toluenesulfonic acid were added and stirred overnight at room temperature. The resulting suspension was filtered, and the residue was washed three times with 5 mL of cold methanol and dried in vacuum ($10^{-3}$ mbar) to yield analytically pure samples of the title compound in 83% yield. $^1$H NMR (400 MHz, $CDCl_3$, 25 °C): $\delta$ . 12.23 (br s, 1H, O*H*), 8.29 (s, 1H), 8.16 (d, $J$ = 3.4, 1H), 7.65 (d, $J$ = 3.4, 1H), 7.66 (d, $J$ = 3.4, 1H), 6.95 (t, $J$ = 8.2).

**6-C(H)═N[2,6-{3,5-$(F_3C)_2C_6H_3$}$_2C_6H_3$]-2,4-{3,5-$(F_3C)_2C_6H_3$}$_2$-$C_6H_2$OH (1a).** To a mixture of 2-((2,6-dibromophenylimino)-methyl)-4,6-diiodophenol (4.9 mmol, 3 g), 6 equiv of 3,5-bis(trifluoromethyl)phenylboronic acid (30 mmol, 7.65 g), 5 mol % $[Pd(dba)_2]$ (0.25 mmol, 142 mg), and 10 mol % $PPh_3$ (0.50 mmol, 130 mg), in an argon-filled Schlenk flask were added 120 mL of toluene, 40 mL of ethanol, and 30 mL of an aqueous 2 M $Na_2CO_3$ solution. The suspension was heated with vigorous stirring to 90 °C for 48 h. The resulting biphasic mixture was stirred for 30 min under air (resulting in formation of palladium black) and poured into a separatory funnel. Water and diethyl ether were added until all salts and organic material dissolved. The aqueous phase was extracted with additional 2 × 50 mL of diethyl ether. The organic phases were combined and filtered through a plug of silica to remove Pd black. After removal of the solvent under vacuum, the product was dissolved in hot methanol and recrystallized slowly from this solution. Yield: 66%.

**Synthesis of 6-C(H)═N[2,4,6-{3,5$(F_3C)_2C_6H_3$}$_3C_6H_2$]-2,4-{3,5-$(F_3C)_2C_6H_3$}$_2C_6H_2$OH (1b).** A solution of 6-C(H)═O-2,4-{3,5-$(F_3C)_2C_6H_3$}$_2C_6H_2$OH (0.55 mmol, 0.30 g), 2,4,6-tris-{3,5-di(trifluoromethyl)phenyl}aniline (0.55 mmol, 0.40 g), and a catalytic amount of *p*-toluenesulfonic acid hydrate in 50 mL of benzene was reflux for 12 h with a Dean-Starck apparatus at 80 °C (bath temperature). The solvent was removed under reduced pressure, 10 mL of methanol was added, and the mixture was stirred under an inert atmosphere for 2 h. The resulting pale brown solid was collected by filtration, washed with small portions of cold methanol, and dried in a vacuum. Yield: 62%. $^1$H NMR (600 MHz, $C_6D_6$): $\delta$ 12.50 (br. s, 1H, O*H*), 7.95 (s, 2H), 7.91 (s, 3H), 7.77 (s, 1H), 7.70 (s, 1H), 7.67 (s, 4H), 7.65 (s, 2H), 7.47 (s, 2H), 7.14 (s, 2H), 7.08 (s, 1H), 6.92 (d, $J$ = 2.0, 1H), 6.53 (d, $J$ = 1.9, 1H). $^{13}$C NMR (151 MHz, $C_6D_6$): $\delta$ 170.26 ($C_q$), 159.09 ($C_q$), 146.13($C_q$), 142.25 ($C_q$), 141.74 ($C_q$), 140.61 ($C_q$), 138.83 ($C_q$), 133.76 (CH), 131.69 (CH), 130.64 ($C_q$), 130.28 (CH), 130.15 ($C_q$), 129.86 (CH), 129.62 (CH), 128.98 ($C_q$), 128.39 (CH), 127.70 (CH), 126.89 (CH), 124.96 ($C_q$), 124.75 ($C_q$), 124.75 ($C_q$), 123.35 ($C_q$), 123.35 ($C_q$), 123.18 ($C_q$), 122.81 ($C_q$), 122.34 (CH), 122.07 (CH), 121.98 (CH), 121.33 (CH). Anal. Calcd for $C_{53}H_{21}F_{30}NO$ ($M_w$ = 1257.69 g mol$^{-1}$): C 50.61, H 1.68, N 1.11. Found: C 51.07, H 1.82, N 0.98.

**General Procedure for the Synthesis of ($\kappa^2$-*N*,*O*)-Salicylaldiminatonickel Methyl Pyridine Complexes.** 5 mL of cold diethyl ether was added to 1.1 equiv of $[(pyridine)_2NiMe_2]$ and the respective salicylaldimine in a 25 mL Schlenk flask under stirring. A slow methane evolution was observed within 15−30 min. The deep red mixture was stirred for an additional 120 min at 25 °C. The solvent was removed in vacuo. The residue was dissolved in a small amount of benzene and filtered trough a syringe filter. The volatiles were removed by sublimation at −10 °C (crushed ice/sodium chloride) under high vacuum ($10^{-3}$ mbar) to afford the pyridine complexes.

**2b-pyr.** Following the above general procedure, 108.8 mg (77.2 mmol, 97%) of compound **2b-pyr** were obtained as a red powder from $[(pyridine)_2NiMe_2]$ (87.5 mmol, 21.6 mg) and **1b**

(79.5 mmol, 100 mg). The 3,5-bis(trifluoromethyl)phenyl groups are not chemically identical, and the large number of fluorine−carbon couplings hampered the assignment of carbon spectra. Nevertheless, the unique and characteristic resonance of the low field shifted Ni-methyl protons with the expected ratio of signal intensity (aromatic vs nickel methyl) evidence the purity of the compound. $^1$H NMR (400 MHz, $C_6D_6$, 25 °C): $\delta$ 7.89 (s, 4H), 7.59 (m, 7H), 7.45 (m, 3H), 7.30 (s, 1H), 7.24 (s, 2H), 6.91 (s, 2H), 6.78 (s, 1H), 6.65 (s, 1H), 6.52 (s, 1H), 6.27 (m, 1H), 5.86 (m, 2H), −1.13 (s, 3H) Anal. Calcd for $C_{59}H_{28}F_{30}N_2NiO$ ($M_w$ = 1409.5 g mol$^{-1}$): C 50.27, H 2.00, N 1.99. Found: C 50.97, H 2.12, N 1.72.

**4-pyr.** Following the general procedure, 69.3 mg (0.16 mmol, 88.8%) of compound **4-pyr** was obtained as a brown powder from [(pyridine)$_2$NiMe$_2$] (0.19 mmol, 48 mg) and **3** (0.18 mmol, 50 mg). Crystals suitable for X-ray diffraction analysis precipitated from the reaction mixture within 5 min at 25 °C. $^1$H NMR (400 MHz, $C_6D_6$, 25 °C): $\delta$ 8.62 (d, $^3J_{HH}$ = 4.8 Hz, 2H, 21 + 25-H), 7.24 (s, 3H, 11−13H), 7.02 (d, $^3J_{HH}$ = 10.6, 1H, 8-H), 6.65 (vt, $J$ = 10.6, 1H, 7-H), 6.54 (vt, $J$ = 6.6, 1H, 23-H), 6.31 (m, 2H, 4 + 5-H), 6.19 (vt, $J$ = 6.5, 2H, 22 + 24−H), 6.10 (m, 1H, 6-H), 3.97 (m, 2H, 15 + 18 −H), 1.59 (d, $^3J_{HH}$ = 6.6, 6H, 16 + 19-H), 1.16 (d, $^3J_{HH}$ = 6.6, 6H, 17 + 20-H), −0.55 (s, 3H, Ni C$H_3$). $^{13}$C NMR (100.5 MHz, $C_6D_6$, 25 °C): $\delta$ 180.3 ($C_q$, C2), 169.8 ($C_q$, C3), 152.1 (CH, C21 + C25), 144.3 ($C_q$, C9), 142.7 ($C_q$, C10 + C14), 135.5 (CH, C23), 134.7 (CH, C7), 132.8 (CH, C5), 126.2 (CH, C12), 124.3 (CH, C11 + C13), 123.4 (CH, C22 + C24), 121.2 (CH, C6), 120.2 (CH, C4), 120.1 (CH, C8), 2835 (CH, C15 + C18), 25.0 (CH, C17 + C20), 24.0 (CH, C16 + C19), −6.2 (CH, Ni$CH_3$).

**General Procedure for the Synthesis of ($\kappa^2$-*N,O*)-Salicylaldiminato Nickel Methyl tmeda Complexes (2a-d-tmeda).** To a benzene solution of [(tmeda)NiMe$_2$] was added 0.95 equiv of the respective salicylaldimine ligand **1a-d** at room temperature. The temperature was raised to room temperature, and the deep red mixture was stirred for 120 min. The solution was filtrated trough a syringe filter to remove decomposed [(tmeda)NiMe$_2$] present in excess. The volatiles were removed by sublimation at −10 °C (crushed ice/sodium chloride) under high vacuum ($10^{-3}$ mbar) to yield the corresponding tmeda complexes **2a-d-tmeda** which were employed as catalyst precurors without characterization.

**Solubility measurements** were carried out as reported previously[19] in a custom-made setup at the LPCM CNRS-UMR 5803 in Bordeaux. Briefly, a magnetically stirred 5.5 cm$^3$ titanium cell with two silicon windows for the infrared (IR) absorption measurements (path length 25 mm) and two sapphire windows for direct observation of the solution to ensure that there is no demixing in the sample were employed. Pressures up to 50 MPa can be adjusted by a hydraulic system via a stainless steel capillary. Single-beam IR spectra were obtained in the spectral range 400−6000 cm$^{-1}$ with 2 cm$^{-1}$ resolution by Fourier transformation of 50 accumulated interferograms acquired with a Biorad FTS-60A interferometer. Spectra were collected at 50 °C at 6−35 MPa. The concentration of the solute was determined employing the Beer−Lambert law from the intensity of characteristic IR bands of the solute. The overall procedure was (1) identification of suitable characteristic vibrational bands, (2) determination of the molar extinction coefficient for these bands, with a small quantity of solute (ca. 2 mg) completely solubilized at 50 °C and 35 MPa ($\rho$ = 0.9 g cm$^{-3}$), and (3) determination of the solubility with an excess of solute from the intensity of the selected bands.

**Polymerizations in supercritical carbon dioxide** were carried out in a high-pressure view cell supplied by NWA GmbH, Lörrach, Germany. The mechanically stirred stainless steel cell with an internal volume of 30−60 cm$^3$ adjustable by means of a piston operated by a hydraulic system is suited up to 100 MPa and 473.15 K. The cell is heated by two stainless steel cartridge heaters located in cavities in the cell wall, controlled by a thermocouple inside the cell. The pressure was measured with a Bourdon-type manometer. Gases were pumped into the cell by high-pressure pumps (PM-101, NWA GmbH) up to the desired pressure (up to 60 MPa for $CO_2$ and up to 40 MPa for ethylene). The rate of the ethylene addition was controlled by a two-way HPLC valve, with an internal loop volume of 1 mL. The quantity of gases introduce was estimated by the piston position and the pressure. Prior to a polymerization experiment, the reactor was heated under a low pressure of $CO_2$ to the desired temperature for 30 min and flushed three times with $CO_2$. The solid catalyst precursor and optionally the comonomer were added via a modified syringe. For polymerization at 50 °C (supercritical state), the reactor was filled with 60 mL of $CO_2$ to the desired pressure (10 MPa), corresponding to ca. 15 g of $CO_2$ (according to ref 26). For polymerization at lower temperatures (liquid state), the reactor was filled with 35 mL (ca. 30 g) of $CO_2$ to the desired pressure (10 MPa). Once the reactor was filled with $CO_2$, the pressure was increased (to 30 MPa) by decreasing the cell volume under continuous stirring. Ethylene was added to the reactor at constant pressure and temperature, increasing the volume of the cell. The increase of the volume was used to roughly estimate the amount of ethylene added, assuming that the added volume corresponds to the density of pure ethylene under the reaction conditions.[26] Polymerizations were carried out at a pressure of 65 MPa, obtained by decreasing the volume of the reactor. The reaction was stopped by increasing the volume of the cell and carefully venting the reactor.

**Table 5. Details of the Crystal Structure Determination of 4-pyr**

| | |
|---|---|
| CCDC deposit no | 737934 |
| formula | $C_{25}H_{30}N_2ONi$ |
| formula weight, g mol$^{-1}$ | 433.22 |
| cryst size, mm | 0.35 × 0.3 × 0.25 |
| space group | $P21/c$ |
| $a$, Å | 15.7604(13) |
| $b$, Å | 8.4707(5) |
| $c$, Å | 16.8054(15) |
| α, deg | 90 |
| $\beta$, deg | 96.515(7) |
| $\gamma$, deg | 90 |
| $V$, Å$^3$ | 2229.1(3) |
| $Z$ | 4 |
| $\delta_{calc}$, g cm$^{-3}$ | 1.291 |
| $T$, K | 100 |
| $\mu$, mm$^{-1}$ | 0.888 |
| $F$(000) | 920 |
| $\Theta_{max}$, deg | 25.73 |
| no. of rflns measd | 28 560 |
| no. of unique rflns | 4218 |
| no. of rflns $I > 2\sigma(I)$ | 3562 |
| $R_1$, $I > 2\sigma(I)^a$ | 0.0461 |
| $R_1$, all data | 0.0588 |
| $wR_2{}^a$ | 0.0828 |
| diff Fourier peak min/max, e Å$^{-3}$ | −0.790/0.367 |

$^a$ $R_1 = \sum||F_o - F_c||/\sum|F_0|$, $wR_2 = [\sum(w(F_o{}^2 - F_c{}^2)^2)/\sum(w(F_o{}^2)^2)]^{1/2}$.

**X-ray Crystal Structure Determination of 4-pyr (Table 5).** The data collection was performed at 100 K on a STOE IPDS-II diffractometer equipped with a graphite-monochromated radiation source ($\lambda$ = 0.710 73 Å) and an image plate detection system. A crystal mounted on a fine glass fiber with silicon grease was employed. The selection, integration, and averaging procedure of the measured reflex intensities, the determination of the unit cell dimensions by a least-squares fit of the 2Θ values, data reduction, LP correction, and space group determination were performed using the X-Area software package delivered with the diffractometer. A semiempirical absorption correction was not performed. The structure was solved by direct methods (SHELXS-97), completed with difference Fourier syntheses, and refined with full-matrix least-squares using SHELXL-97 minimizing $w(F_o{}^2 - F_c{}^2)^2$. Weighted $R$ factor ($wR$) and the goodness of fit $S$ are based on $F^2$; the conventional $R$ factor ($R$) is based on $F$. All non-hydrogen atoms were refined with anisotropic displacement parameters. All scattering factors

and anomalous dispersion factors are provided by the SHELXL-97 program. All hydrogen atom positions were calculated geometrically and were allowed to ride on their parent carbon atoms with fixed isotropic $U_{11} = 0.02$.

**Acknowledgment.** Financial support by the BMBF (project 03X5505) is gratefully acknowledged. We thank Thierry Tassaing and the LPCM CNRS-UMR 5803 in Bordeaux for access to the high-pressure cell for solubility measurements. TEM studies were carried out by Marina Krumova and GPC analyses by Lars Bolk. S.M. is indebted to the Fonds der Chemischen Industrie and to the Hermann-Schnell Foundation.

**Supporting Information Available:** Complete structural data of **4-pyr** (CIF file). This material is free of charge via the Internet at http://pubs.acs.org.

## References and Notes

(1) (a) *Chemical Synthesis Using Supercritical Fluids*; Jessop, P. G., Leitner, W., Eds.; Wiley-VCH: Weinheim, 1999. (b) Leitner, W. *Acc. Chem. Res.* **2002**, *35*, 746–756. (c) *Supercritical Carbon Dioxide in Polymer Reaction Engineering*; Kemmere, M. F., Meyer, T., Eds.; Wiley-VCH: Weinheim, 2005.

(2) (a) Kendall, J. L.; Canelas, D. A.; Young, J. L.; DeSimone, J. M. *Chem. Rev.* **1999**, *99*, 543–563. (b) Wells, S. L.; DeSimone, J. M. *Angew. Chem.* **2001**, *113*, 534–544. (c) *Angew. Chem., Int. Ed.* **2001**, *40*, 518−527

(3) DeSimone, J. M.; Guan, Z.; Elsbernd, C. S. *Science* **1992**, *257*, 945–947.

(4) Biddulph, R. H.; Plesch, P. H. *J. Chem. Soc.* **1960**, *82*, 3913–3920.

(5) (a) Darensbourg, D. J.; Stafford, N. W.; Katsurao, T. *J. Mol. Catal. A* **1995**, *104*, L1–L4. (b) Costello, C. A.; Berluche, E.; Han, S. J.; Sysyn, D. A.; Super, M. S.; Beckman, E. J. *Polym. Prepr.* **1996**, *74*, 430. (c) Duper, M.; Berluche, E.; Costello, C.; Beckman, E. *Macromolecules* **1997**, *30*, 368–372.

(6) (a) Klaui, W.; Bongards, J.; Reib, G. J. *Angew. Chem.* **2000**, *112*, 4077–4079. (b) *Angew. Chem., Int. Ed.* **2000**, *39*, 3894−3896

(7) Hori, H.; Six, C.; Leitner, W. *Macromolecules* **1999**, *32*, 3178–3182.

(8) (a) Fürstner, A.; Ackermann, L.; Beck, K.; Hori, H.; Koch, D.; Langemann, K.; Liebl, M.; Six, C.; Leitner, W. *J. Am. Chem. Soc.* **2001**, *123*, 9000–9006. (b) Fürstner, A.; Koch, D.; Langemann, K.; Leitner, W.; Six, C. *Angew. Chem.* **1997**, *109*, 2562–2565. (d) *Angew. Chem., Int. Ed. Engl.* **1997**, *36*, 2466−2469. (c) Mistele, C. D.; Thorp, H. H.; DeSimone, J. M. *J. Macromol. Sci., Part A* **1996**, *33*, 953–960.

(9) Killian, C. M.; Johnson, L. K.; Brookhart, M. *J. Am. Chem. Soc.* **1995**, *117*, 6414–6415.

(10) (a) Johnson, L. K.; Killian, C. M.; Arthur, S. D.; Feldman, J.; McCord, E. F.; McLain, S. J.; Kreutzer, K. A.; Bennett, M. A.; Coughlin, E. B.; Ittel, S. D.; Parthasarathy, A.; Tempel, D. J.; Brookhart, M. S. WO 96/23010, DuPont; University of North Carolina, **1996**. (b) De Vries, T. J.; Duchateau, R.; Vorstman, M. A. G.; Keurentjes, J. T. F. *Chem. Commun.* **2000**, 263–264. (c) De Vries, T. J.; Kemmere, M. F.; Keurentjes, J. T. F. *Macromolecules* **2004**, *37*, 4241–4246. (d) Kemmere, M.; De Vries, T. J.; Keurentjes, J. In *Supercritical Carbon Dioxide in Polymer Reaction Engineering*; Kemmere, M. F., Meyer, T., Eds.; pp 157−187.

(11) Bastero, A.; Franciò, G.; Leitner, W.; Mecking, S. *Chem.—Eur. J.* **2006**, *12*, 6110–6116.

(12) Early work: (a) Keim, W.; Kowaldt, F. H.; Goddard, R.; Krüger, C. *Angew. Chem., Int. Ed. Engl.* **1978**, *17*, 466–467. (b) Ostoja Starzewski, K. A.; Witte, J. *Angew. Chem., Int. Ed. Engl.* **1985**, *24*, 599–601. (c) Klabunde, U.; Ittel, S. D. *J. Mol. Catal.* **1987**, *41*, 123–134.

(13) (a) Wang, C.; Friedrich, S.; Younkin, T. R.; Li, R. T.; Grubbs, R. H.; Bansleben, D. A.; Day, M. W. *Organometallics* **1998**, *17*, 3149–3151. (b) Johnson, L. K.; Bennett, A. M. A.; Ittel, S. D.; Wang, L.; Parthasarathy, A.; Hauptman, E.; Simpson, R. D.; Feldman, J.; Coughlin, E. B. WO98/30609, DuPont, **1998**. (c) Younkin, T. R.; Connor, E. F.; Henderson, J. I.; Friedrich, S. K.; Grubbs, R. H.; Bansleben, D. A. *Science* **2000**, *287*, 460–462. (d) Hicks, F. A.; Brookhart, M. *Organometallics* **2001**, *20*, 3217–3219. (e) Soula, R.; Broyer, J. P.; Llauro, M. F.; Tomov, A.; Spitz, R.; Claverie, J.; Drujon, X.; Malinge, J.; Saudemont, T. *Macromolecules* **2001**, *34*, 2438–2442. (f) Gibson, V. C.; Tomov, A.; White, A. J. P.; Williams, D. J. *Chem. Commun.* **2001**, 719–720. (g) Zuideveld, M.; Wehrmann, P.; Röhr, C.; Mecking, S. *Angew. Chem., Int. Ed.* **2004**, *43*, 869–873. (h) Jenkins, J. C.; Brookhart, M. *J. Am. Chem. Soc.* **2004**, *126*, 5827–5842. (j) Zhang, L.; Brookhart, M.; White, P. S. *Organometallics* **2006**, *25*, 1868–1874. (k) Kuhn, P.; Sémeril, D.; Jeunesse, C.; Matt, D.; Neuburger, M.; Mota, A. *Chem.—Eur. J.* **2006**, *12*, 5210–5219. (l) Göttker-Schnetmann, I.; Wehrmann, P.; Röhr, C.; Mecking, S. *Organometallics* **2007**, *26*, 2348–2362. (m) Yu, S.-M.; Berkefeld, A.; Göttker-Schnetmann, I.; Müller, G.; Mecking, S. *Macromolecules* **2007**, *40*, 421–428. (n) Bastero, A.; Göttker-Schnetmann, I.; Röhr, C.; Mecking, S. *Adv. Synth. Catal.* **2007**, *349*, 2307–2316.

(14) (a) Ittel, S. D.; Johnson, L. K.; Brookhart, M. *Chem. Rev.* **2000**, *100*, 1169–1203. (b) Gibson, V. C.; Spitzmesser, S. K. *Chem. Rev.* **2003**, *103*, 283–316. (c) Mecking, S. *Coord. Chem. Rev.* **2000**, *203*, 325–351. (d) Mecking, S. *Angew. Chem., Int. Ed.* **2001**, *40*, 534–540. (e) Guan, Z. *Chem.—Eur. J.* **2002**, *8*, 3086–3092. (f) Domski, G. J.; Rose, J. M.; Coates, G. W.; Bolig, A. D.; Brookhart, M. *Prog. Polym. Sci.* **2007**, *32*, 30–92. (g) Berkefeld, A.; Mecking, S. *Angew. Chem., Int. Ed.* **2008**, *47*, 2538–2542.

(15) Bauers, F. M.; Mecking, S. *Angew. Chem., Int. Ed.* **2001**, *40*, 3020–3022.

(16) Berkefeld, A.; Mecking, S. *J. Am. Chem. Soc.* **2009**, *131*, 1565–1574.

(17) Perfluoroalkyl-substituted salicylaldehyde has been previously prepared by a five-step synthesis: Pozzi, G.; Cinato, F.; Montanari, F.; Quici, S. *Chem. Commun.* **1998**, 877–878.

(18) Wehrmann, P.; Mecking, S. *Macromolecules* **2006**, *39*, 5995–6002.

(19) For a detailed description of the setup and method employed, cf. Supporting Information of: Martinez, V.; Mecking, S.; Tassaing, T.; Besnard, M.; Moisan, S.; Cansell, F.; Aymonier, C. *Macromolecules* **2006**, *39*, 3978–3979.

(20) Bastero, A.; Kolb, L.; Wehrmann, P.; Bauers, F. M.; Göttker gen. Schnetmann, I.; Monteil, V.; Thomann, R.; Chowdhry, M. M.; Mecking, S. *Polym. Mater. Sci. Eng.* **2004**, *90*, 740–741.

(21) Berkefeld, A.; Möller, H. M.; Mecking, S. *Organometallics* **2009**, *28*, 4048–4055.

(22) Analogous reaction of [(tmeda)$NiMe_2$] with enolatoimine **5** failed to afford **6-tmeda**.

(23) Polymerization of ethylene in toluene at 50 °C under 40 bar of ethylene pressure with 10 $\mu$mol of **4-pyr** for 60 min afforded 7.12 g of polyethylene corresponding to TO $h^{-1}$ = 25 000, $M_w$ = 935 500, $M_w/M_n$ = 2.2, $T_m$ = 116 °C, $\chi$ = 37%.

(24) The solubility of the catalyst precursor could be visualized via the sapphire window of the autoclave.

(25) Wehrmann, P.; Mecking, S. *Organometallics* **2008**, *27*, 1399–1408.

(26) http://webbook.nist.gov/chemistry/fluid/.

(27) Joo, Y. L.; Han, O. H.; Lee, H.-K.; Song, J. K. *Polymer* **2000**, *41*, 1355–1368.

(28) (a) Phillips, R. A. *J. Polym. Sci., Part B: Polym. Phys.* **1998**, *36*, 495. (b) Kresteva, M.; Nedkov, E.; Radilova, A. *Colloid Polym. Sci.* **1985**, *263*, 273. (c) Höhne, G. W. H. *Polymer* **2002**, *43*, 4689 and references therein.

(29) Whiteley, K. S.; Heggs, T. G.; Koch, H.; Mawer, R. L.; Immel, W. I. In *Ullmann's Encyclopedia of Industrial Chemistry*, 6th ed.; Wiley-VCH: Weinheim, 2003; Vol. *28*, p 400.

(30) For densities of similar polyethylenes obtained by late transition metal catalysis, cf.: Meinhard, D.; Wegner, M.; Kipiani, G.; Hearley, A.; Reuter, P.; Fischer, S.; Marti, O.; Rieger, B. *J. Am. Chem. Soc.* **2007**, *129*, 9182–9191.

(31) Connor, E. F.; Younkin, T. R.; Henderson, J. I.; Hwang, S. J.; Roberts, W. P.; Litzau, J. J.; Grubbs, R. H. *J. Polym. Sci., Part A* **2002**, *40*, 2842–2854.

(32) (a) Makovetsky, K. L.; Finkelstein, E. S.; Bykov, V. I.; Bagdasaryan, A. K.; Goodall, B. L.; Rhodes, L. F. WO98/56837, B.F. Goodrich, **1998**. (b) Benedikt, G. M.; Elce, E.; Goodall, B. L.; Kalamarides, H. A.; McIntosh, L. H.; Rhodes, L. F.; Selvy, K. T. *Macromolecules* **2002**, *35*, 8969–8977. (c) Kiesewetter, J.; Kaminsky, W. *Chem.—Eur. J.* **2003**, *9*, 1750–1758.

(33) For example, nickel alkyl complexes can insert carbon dioxide to afford a nickel propionate complex, which would likely be inactive for insertion polymerization. (a) Kreher, U.; Schebesta, S.; Walther, D. *Z. Anorg. Allg. Chem.* **1998**, *624*, 602–612. (b) Yamamoto, T.; Yamamoto, A. *Chem. Lett.* **1978**, *6*, 615–616.

(34) Kaschube, W.; Pörschke, K. R.; Wilke, G. *J. Organomet. Chem.* **1988**, *355*, 525–532.

(35) Càmpora, J.; Conejo, M. d. M.; Mereiter, K.; Palma, P.; Pérez, C.; Reyes, M. L.; Ruiz, C. *J. Organomet. Chem.* **2003**, *683*, 220–239.

(36) Hicks, F. A.; Brookhart, M. *Org. Lett.* **2000**, *2*, 219–221.